Research Article

Received: 8 June 2022 Revised: 22 July 2022 Accepted article published: 26 July 2022 Published online in Wiley Online Library: 13 August 2022

(wileyonlinelibrary.com) DOI 10.1002/jctb.7197

Effective removal of methylene blue dye by a novel 4-vinylpyridine-co-methacrylic acid cryogel: kinetic, isotherm, and breakthrough studies

Harry Kwaku Megbenu,[a] Zhandos Tauanov,[c] Chingis Daulbayev,[b] Stavros G. Poulopoulos[a*] and Alzhan Baimenov[b,c*]

Abstract

BACKGROUND: Industrial streams are the source of increasing amounts of textile dye pollution every year. Among the various adsorbents that have been tested for the removal of dyes, synthetic macroporous polymers are a promising choice due to their developed structure, the presence of active functional groups, and the possibility of regeneration and reuse for several cycles. In this work, a 4-vinylpyridine-co-methacrylic acid based cryogel (4-VP-MAAc) was synthesized at -12 °C by the free-radical polymerization technique, it was characterized using a set of complimentary methods, and then applied for the removal of methylene blue (MB) from water solutions.

RESULTS: The adsorption of MB was enhanced at pH values higher than 7 due to the presence of anionic functional groups. The maximum equilibrium adsorption capacity achieved by 4-VP-MAAc was 703.6 mg/g at pH 8. Several kinetics, equilibrium, pH studies, and fixed-bed column experiments were completed in ultra-pure water to evaluate the performance and the mechanism of interaction of positively-charged dye with the polymer. Among the kinetic models applied, the pseudo-second order model best fit the experimental observations. The Langmuir model efficiently described the adsorption of MB onto the prepared cryogel, thus indicating monolayer adsorption. The ion exchange of the Na^+ ions present in the structure of the cryogel with dye was found to be the main removal mechanism accompanied with a complexation reaction. No loss of adsorption capacity was observed in four successive adsorption/desorption cycles of 4-VP-MAAc use.

CONCLUSION: This is the first time that a 4-vinylpyridine-co-methacrylic acid based cryogel has been synthesized and successfully applied to remove MB from water.

Keywords: cryogels; methylene blue; 4-VP-MAAc; textile dye pollution; ion exchange

INTRODUCTION

A large number of synthetic dyes has been widely used in the textile, pharmaceutical, cosmetic, rubber, paper, plastic, leather, and food industries in recent years.[1] As a result, large amounts of these dyes are discharged into waste effluents without proper treatment, thus contributing to the water pollution problems faced by today's society.[2,3] The disposal of these colored wastes into water bodies does not only negatively affect their recreational use, but it also inhibits sunlight transmission in the water, leading to the reduction of photosynthetic activities.[4] While most synthetic dyes are known to be toxic, methylene blue (MB), a cationic dye', poses a higher risk to human health and the environment due to its physical and chemical properties.[5] Specifically, exposure to MB can cause a rise in heart rate, excessive vomiting, cyanosis, shock, jaundice, tissue necrosis, quadriplegia, and Heinz body formation in humans.[6] Dyes, in general, exhibit a synthetic and complex nature because they are designed to withstand certain conditions, such as exposure to sunlight, soap, water, and oxidizing agents; therefore, they cannot be easily removed by conventional methods for wastewater treatment.[7] Consequently, various techniques, such as coagulation,[8] photodecomposition,[9] flocculation,[10] adsorption,[11] ion exchange,[12] and chemical oxidation,[13] have been applied to remove these pollutants from water. Among these methods, adsorption is one of the physico-chemical methods that is most widely used due to its economic benefits,

* Correspondence to: Dr. S. G. Poulopoulos, Chemical and Materials Engineering Department, School of Engineering and Digital Sciences, Nazarbayev University, Nur-Sultan, Kazakhstan. E-mail: stavros.poulopoulos@nu.edu.kz; or Dr. A. Baimenov, National Laboratory Astana, Nazarbayev University, Nur-Sultan, Kazakhstan, E-mail: alzhan.baimenov@nu.edu.kz

a Chemical and Materials Engineering Department, School of Engineering, Nazarbayev University, Nur-Sultan, Kazakhstan

b National Laboratory Astana, Nazarbayev University, Nur-Sultan, Kazakhstan

c Faculty of Chemistry and Chemical Technology, Al-Farabi Kazakh National University, Almaty, Kazakhstan

variety of adsorbents, ease of operation, adsorbent reusability, and environmentally friendly nature.[14] Adsorption of dyes by nano- and macroporous particles, bulk materials, and membranes from wastewater is based on the use of several materials, such as polymers,[15] activated carbon,[16] zeolite,[17] and clays,[18] as well as industrial and agricultural wastes.[19]

Polymeric materials, such as cryogels, have attracted great interest due to their outstanding physico-chemical properties.[20] Cryogels are cryogenically-designed polymeric materials with diverse applications in environmental engineering, tissue engineering, medicine, food technology, and biology.[20,21] They are synthesized *via* several methods, including free radical polymerization, polycondensation reaction, self-assembly based gelation, enzymatic catalysis, and ionic interaction; they also contain a three-dimensional (3D) structure that is flexible. Cryogels normally contain specific functional groups, like hydroxyl, carboxylic, amine, amide, and thiol, that enable them to effectively adsorb pollutants into their structure from water. They have been effectively utilized in the adsorption of cationic dyes due to their low cost, relative ease of processing and regeneration, high recovery efficiency, environmentally friendly nature, highly abundant active sites, and good mechanical properties.[22-24]

In this work, a novel macroporous cryogel containing 4-vinylpyridine and methacrylic acid as main monomers (named 4VP-MAAc) with attractive physicochemical properties was synthesized by the free radical polymerization technique under sub-zero temperature. Surface characterization and functional group determination techniques were employed to evaluate the physico-chemical parameters of 4VP-MAAc. The adsorption capacity of the synthesized cryogel was estimated in the adsorption of MB from water. Various models were applied to evaluate the removal behavior. This is the first time that a cryogel of such composition was synthesized, fully characterized and used for the removal of methylene blue dye from water invarious experimental conditions.

MATERIALS AND METHODS

Materials

4-vinylpyridine (4-VP) was purchased from Sigma-Aldrich (Germany) and purified to remove hydroquinone (inhibitor) before being used for synthesis. Methacrylic acid (MAAc), Dimethylacrylamide (DMAAm), N,N,N′,N′-tetramethyl ethylene diamine (TEMED), N,N′-methylenebisacrylamide (BisAAm), sodium hydroxide (NaOH), and ammonium persulfate (APS) were purchased from Sigma-Aldrich and used as received. Methylene blue (MB) dye, with a molecular weight of 319.85 g/mol, was purchased from Acros Organics (New Jersey, USA).

Synthesis of 4-vinylpyridine methacrylic acid cryogel

The cryogel synthesis followed a free-radical polymerization technique.[25] For a typical synthesis route, 4-VP and MAAc were used as the main monomers, while BisAAm was used as a cross-linker, DMAAm as a precursor of functional groups, and TEMED and APS as catalyzer and initiator, respectively. 4-VP was purified by vacuum distillation at 100 °C and 150 kPa to remove the hydroquinone.

The synthesis of the cryogel was performed as follows: 20 mL of deionized water was degassed by purging nitrogen gas for about 30 min. BisAAm (0.23 g) was added under continuous stirring to allow complete dissolution, followed by addition of 0.246 mL of MAAc and 0.309 mL of DMAAm. 0.319 mL of pure 4-VP was added under vigorous stirring, which was accompanied by acid neutralization by means of 5 M NaOH (0.55 mL) to obtain a pH in the range of 6.5–7.5. After obtaining a homogenous solution from the above mixture, 0.05 mL TEMED was added dropwise and 5% APS (0.80 mL) was added to initiate the polymerization process. 2 mL of the final mixture was measured into clean plastic syringes that had already been placed in the heating–cooling thermostat circulating system (Julabo F34, Germany) at −12.0 °C. The reaction mixture was left in the cooling bath for 24 h for complete polymerization to take place.

The synthesized cryogel was then washed several times with ultrapure water and with a 50% ethanol solution to remove any unreacted monomers from the monoliths. The washed cryogel was freeze dried with a tabletop freeze dryer (FreeZone 2.5 L, Labconco) at -54 °C and 50 kPa pressure for 24 h. The obtained dried cryogel was finally placed in a sealed plastic container for further analysis and use.

Characterization of synthesized cryogel

The morphological and physico-chemical structures of the synthesized cryogel were characterized by Fourier Transform Infrared Spectroscopy (FT-IR). Infrared spectra were recorded in the range of 4000–400 cm^{-1} with a resolution of 4 cm^{-1} and a scanning speed of 1 cm^{-1} s^{-1}, using a Cary 600 Series FTIR spectrophotometer (Agilent Technologies) equipped with an attenuated total reflection (ATR) module. For characterizing the morphological and elemental compositions of the sample, a Zeiss Crossbeam 540 Scanning Electron Microscope (SEM) at 5 kV, equipped with a backscattered electron detector and coupled with Energy-Dispersive X-ray (EDX) spectrometer, was used. Zeta potential of the cryogel was studied by the batch equilibration method. Specifically, 10 mg of cryogel was placed in 10 mL of DI water at an initial pH range of 1–10. The pH was adjusted using 0.1 M NaOH or HCl, while the ionic strength was kept constant. The solutions were placed on a mechanical shaker (Rotamax 120, Heidolph) and left to reach equilibrium for 24 h at room temperature. The zeta potential was measured using Zetasizer Nano (Malvern, UK) instrument. To monitor the release of sodium ion (Na^+) into the mixture, atomic absorption spectrometry (AAS) (AAnalyst 400, Perkin-Elmer, USA) analysis was conducted. Prior to analysis, 1% cesium chloride (CsCl) was prepared by dissolving 1 g of CsCl in 1 L DI water and this was used in the dilution of mixtures due to its higher concentration of Na^+.

Swelling capacity of cryogel

To check the swelling capacity of cryogels, S, 10 mm diameter slices of monoliths were carefully cut and used. The mass of a dry monolith was noted before dissolving each monolith in DI water. The swelling degree percentage was determined by subtracting the mass of the dry monolith from that of the wet monolith and dividing by the mass of the dry monolith, according to Eqn (1) below:[26]

$$S\,(\%) = \frac{w_t - w_o}{w_o} \times 100 \qquad (1)$$

where $w_o\,(g)$ denotes the mass of the dry monolith and $w_t\,(g)$, the mass of wet monolith. The cryogel was withdrawn from the water at specific time intervals and its surface was gently wiped to get rid of excess water before weighing to obtain the mass of

the wet cryogel, w_t (g). This procedure was repeated until the weight remained constant.

Effect of pH

To investigate the effect of pH on the MB adsorption capacity of the synthesized 4VP-MAAc, 10 mg of cryogel was dissolved in 100 mL of a 50 mg/L MB solution at different values of pH (1 to 10). The pH was adjusted with 0.1 M KOH and 0.1 M HCl. After adjusting to the desired pH, solution mixtures were left on the mechanical shaker at 100 rpm for 3 h before measuring the residual MB concentrations. All experiments were done in duplicate.

Batch adsorption kinetics

A volume of 100 mL of 50 mg/L MB solution without pH adjustment (initial pH 8.1) was prepared in a 200 mL beaker. 10 mg powdered cryogel was added in the solution and carefully stirred at 50 rpm for an hour, while monitoring the MB removal. To determine the MB removal with respect to time, about 1 mL of the sample mixture was periodically withdrawn and sent for ultraviolet visible spectrophotometric analysis (UV–vis PhotoLab 6600, WTW GmbH). Prior to analysis, a five-point (0.5, 1, 2.5, 5, and 10 mg/L) calibration curve was prepared for MB solutions at the wavelength of 664 nm. The residual MB concentration was calculated from the general equation obtained from the calibration curve. The adsorption capacity was calculated from Eqn (2) below:

$$q_t = \frac{C_o - C_t}{m} * V \tag{2}$$

where C_t (mg/L) represents the concentration of dye in aqueous solution with respect to time (min), C_o (mg/L) is the initial dye concentration, m (mg) is the mass, and V (L) denotes the total volume used. All experiments were conducted in duplicate and the standard deviations are presented.

To further study the mechanism of removal, the pseudo-first/second order and pseudo-second-order models were applied to fit the experimental data. The linear forms of these models are as follows:[27,28]

$$\ln(q_e - q_t) = \ln q_e - k_1 t \tag{3}$$

$$\frac{t}{q_t} = \frac{1}{k_2 q_e^2} + \frac{t}{q_e} \tag{4}$$

where q_e and q_t are the amount (mg/g) of MB adsorbed at equilibrium and at time t (min), respectively. The pseudo-first order constant k_1 (min^{-1}) and q_e^{cal} can be obtained from the slope and intercept of the $\ln(q_e^{exp} - q_t)$ *versus* time graph. The pseudo-second order constant k_2 (g mg^{-1} min^{-1}) and q_e^{cal} can be calculated from the t/q_t *versus* time graph.

Batch adsorption isotherm

A measured amount of 10 mg of 4VP-MAAc cryogel was mixed with 10 mL of MB solution at different initial concentrations ranging from 1–500 mg/L in 15 mL plastic tubes. The solutions were placed on a mechanical shaking system (Rotamax 120, Heidolph) operating at room temperature and 100 rpm. Samples were periodically withdrawn and the residual MB concentration was measured until the maximum value of MB removal by cryogel was observed. The amount of the adsorbed dye by the cryogel was calculated from Eqn (5):

$$q_{max} = \frac{(C_i - C_{eq})V}{m} \tag{5}$$

where q_{max} (mg/g) denotes the maximum adsorption capacity (mg/g), C_i and C_{eq} represent the initial and equilibrium MB concentrations (mg/L), respectively, V represents the total solution volume (mL), and m represents the total mass (g) of cryogel used. Adsorption isotherm experiments were conducted in duplicate.

Langmuir and Freundlich isotherm models were applied to fit the experimental data to examine the MB adsorption behavior on both homogeneous and heterogeneous surfaces. The linearized form of Langmuir isotherm[28,29] is expressed in Eqn (6):

$$\frac{C_{eq}}{q_{eq}} = \frac{1}{q_{max} K_L} + \frac{C_{eq}}{q_{max}}, \quad R_L = \frac{1}{1 + C_0 * K_L} \tag{6}$$

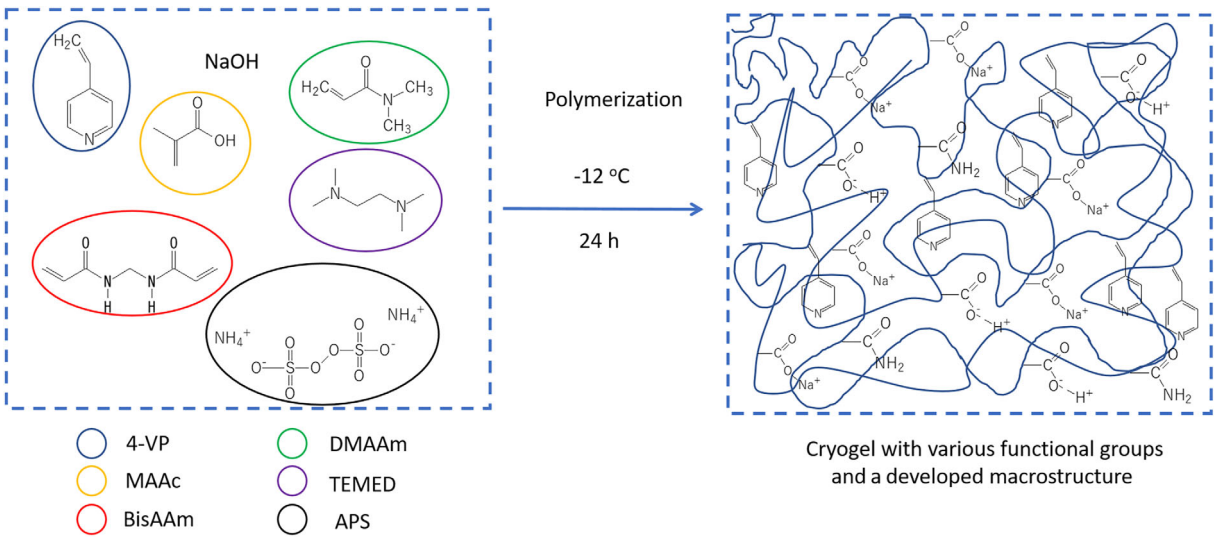

Figure 1. Formation of 4-VP-MAAc cryogel.

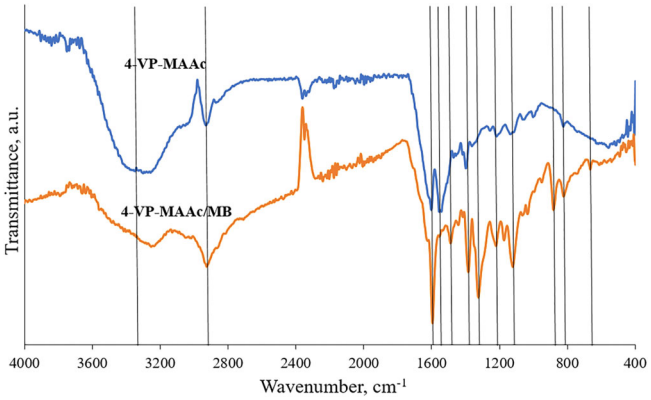

Figure 2. FT-IR spectra of the 4-VP-MAAc cryogel before and after MB removal.

where C_{eq} (mg/L) is the equilibrium concentration of MB in the aqueous phase, q_{eq} and q_{max} (mg/g) are the equilibrium and maximum MB loadings on the cryogel, respectively, and K_L (L/mg) is the Langmuir constant. R_L is a separation factor, while C_0 is the initial concertation of MB. The linear form of Freundlich isotherm is as follows:[30]

$$\log q_{eq} = \log K_F + \frac{1}{n}\log C_{eq} \quad (7)$$

where C_{eq} (mg/L) and q_{eq} (mg/g) are the concentration of MB in the solution and equilibrium adsorption capacity, respectively, while n (dimensionless) and K_F are constants (units depend on the 1/n).

Fixed-bed column experiment

For dynamic study, 34.4 mg of 4VP-MAAc monolith (with length 1 cm and diameter 0.9 cm) was placed in a vertical tube and 400 mL volume of 50 mg/L MB solution was circulated through the cryogel using a peristaltic pump (LOIP LS-301) at the rate of 8 mL/min. The absorbance of the residual MB dye concentration was measured at different time intervals between 1 and 50 min and the residual concentrations were determined from the calibration curve. All experiments were conducted in duplicate.

Three simplified models, namely the Thomas, Yoon–Nelson, and Adams–Bohart models, were adopted to fit the breakthrough data. The Thomas model is one of the most widely used to predict column performances and it is expressed by Eqn (8):

$$\frac{C(t)}{C_0} = \frac{1}{1+\exp\left(\frac{k_{Th}q_{eq}m}{F} - k_{Th}C_0 t\right)} \quad (8)$$

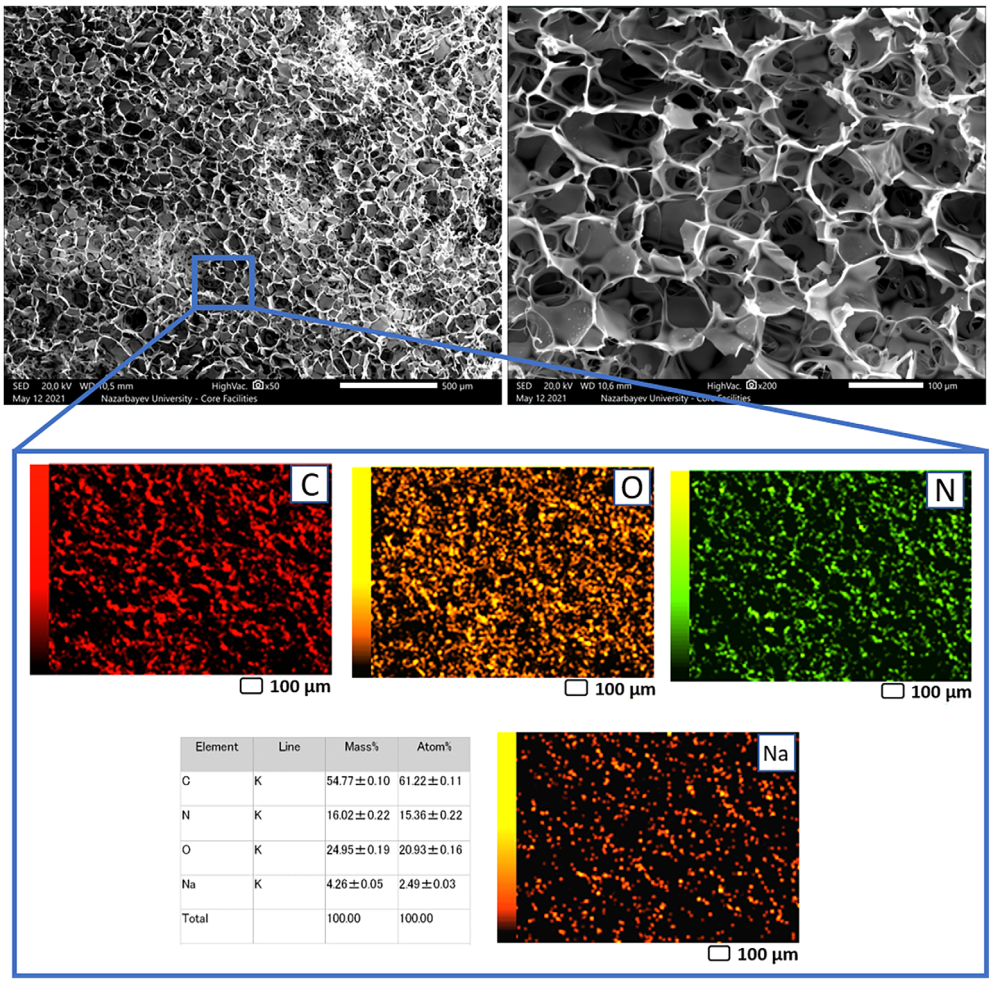

Figure 3. SEM and elemental composition according to EDS mapping technique.

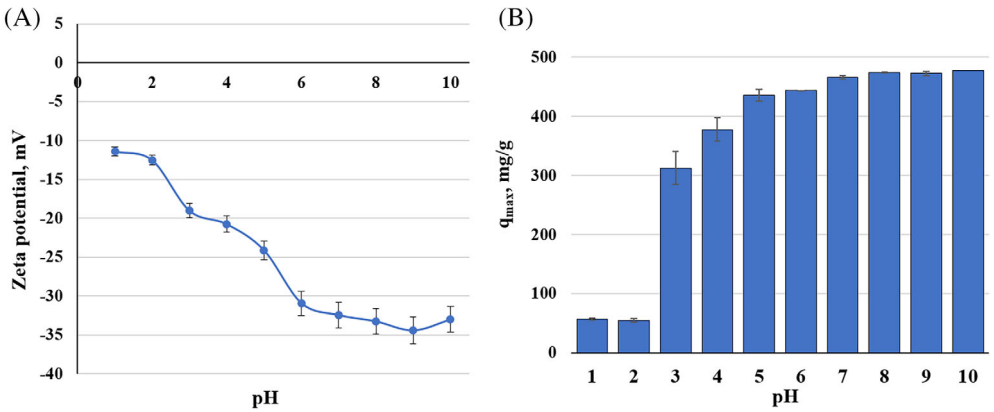

Figure 4. Zeta potential measurements (A) and the maximum adsorption capacity (B) at various pH values.

where C_0 (mg/L) is initial MB concentration and C(t) (mg/L) is concentration at specific time t (min), m is the mass of the cryogel (mg), F is the volumetric flow rate (mL/min), k_{Th} (mL/mg min) is the Thomas rate constant, and q_{eq} (mg/g) is the equilibrium MB uptake per g of the cryogel.

The Yoon-Nelson's model (Eqn (9)) does not require detailed data about neither the characteristics of the adsorbate, the type of adsorbent, nor the physical proportions of the adsorption bed:

$$\frac{C(t)}{C_0} = \frac{\exp[k_{YN}(t-\tau)]}{1+\exp[k_{YN}(t-\tau)]} \tag{9}$$

where C_0 (mg/L) is initial MB concentration and C(t) (mg/L) is concentration at specific time t (min), k_{YN} (mL/min) is the Yoon-Nelson's rate constant, and τ (min) is time when $C(t)/C_0$ is 0.5.

The Adams–Bohart model is based on the assumption that the rate of adsorption is proportional to both the concentration of the adsorbing species and the residual capacity of the adsorbent. It is only used for the description of the initial part of the breakthrough curve and it is expressed in the linear form of Eqn (10):

$$\ln\left[\frac{C(t)}{C_0}\right] = k_{AB}C_0 t - k_{AB}N\frac{H}{U_0} \tag{10}$$

where C_0 (mg/L) is initial MB concentration and C(t) (mg/L) is concentration at specific time t (min), k_{AB} (mL/mg min) is the Adams–Bohart's rate constant, H (cm) is a column height, N (mg/L) is saturation concentration, and U_0 (cm/min) is MB solution flow velocity. A linear relationship between $\ln\left[\frac{C(t)}{C_0}\right]$ and time is obtained for a relative concentration up to $\frac{C(t)}{C_0} = 0.5$, and thus, the values of N and k_{AB} were calculated as intercept and slope of the $\ln\left[\frac{C(t)}{C_0}\right]$ *vs.* t line.

Regeneration/reusability of cryogel

The possibility of regenerating the cryogel after adsorption experiments and reuse it was also studied. Specifically, after each MB adsorption step, the used cryogel was first washed with 100 mL DI water, then washed with 100 mL of 0.1 M HNO_3 solution, followed by 100 mL of water, 100 mL of 0.1 M NaOH, and finally another 100 mL DI water. The reusability of the as-regenerated cryogel was investigated in four successive adsorption–desorption cycles and the regeneration capacity was calculated for each cycle by Eqn (11):

$$R_g\% = \frac{C_o - C_r}{C_o - C_i} * 100 \tag{11}$$

where R_g denotes the regeneration capacity (%), C_o denotes the initial concentration, C_i and C_r represent the residual concentrations of MB dye in solution (mg/L) after initial and regeneration cycles, respectively.

RESULTS AND DISCUSSION

Synthesis and characterization

The ratio of monomers, along with the amount of the cross-linking agent, initiator, and catalyst, are all crucial parameters for the polymerization reaction and for the successful formation of cryogels. For example, an insufficient amount of the cross-linking agent BisAAm leads to a cryogel with a loose structure. The general scheme for the synthesis and formation of the 4-VP-MAAc cryogel is shown in Fig. 1. According to this scheme, 4-VP, MAAc and DMAAm co-polymerize by crosslinking with BisAAm to form the interconnected structure of the polymer. Due to the availability of various functional groups, the synthesized cryogel

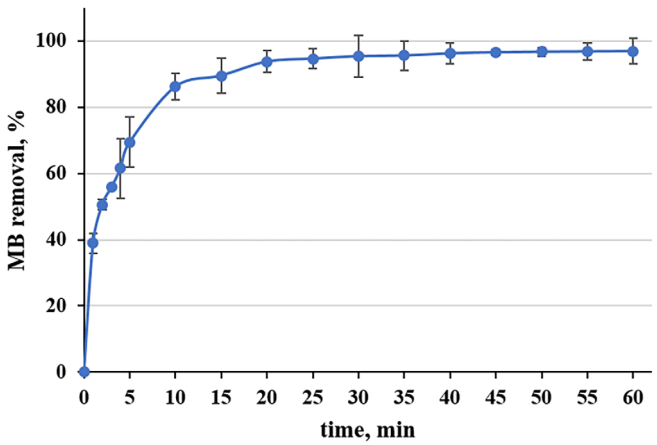

Figure 5. Removal of MB by 4-VP-MAAc cryogel *vs.* time.

Table 1. Parameters of kinetic models for adsorption of MB by 4-VP-MAAc cryogel

Model name	Unit	Values
Experimental data	q_{eq}^{exp} (mg/g)	516.1
Pseudo-first order	q_{eq}^{cal} (mg/g)	257.4
	K_1 (min^{-1})	1.8×10^{-3}
	R^2	0.9865
Pseudo-second order	q_e^{cal} (mg/g)	526.3
	K_2 (g/mg min)	1.0×10^{-3}
	R^2	0.9998

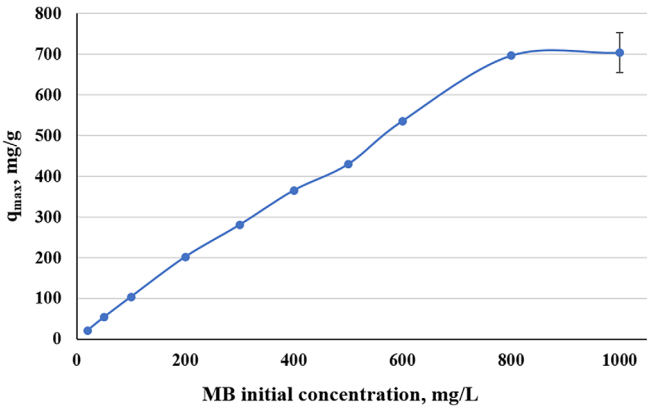

Figure 6. Isotherm of MB removal by 4-VP-MAAc cryogel.

contained carboxylic, amide, and pyridine groups, as well as their derivatives, and others.

To determine the existing functional groups in the cryogel structure, the FT-IR spectra were obtained and shown in Fig. 2.

The peak at ~3300 cm^{-1} refers to the stretching vibrations of -OH groups, while the sharp peak at 2927 cm^{-1} corresponds to C—H stretching bands. For single bonds of -CH-, -CH_2-, and -CH_3-, the absorption spectra are in the region of 2026 cm^{-1}, 2167 cm^{-1}, and 2358 cm^{-1}, respectively. Double asymmetry peaks at 1600 and 1542 cm^{-1} were associated with amide(I) and amide(II) groups, respectively.[31] An absorption peak at 1398 cm^{-1} arises due to the -OH bending of carboxylic acid group. The stretching vibrations bands of C-O-C and C-OH groups are observed at 1217 cm^{-1}, 1132 cm^{-1}, and 1051 cm^{-1}.[32]

According to the SEM microphotographs, the super-macropores (sizes ranging from 10 to 75 μm) with interconnected channels formed a 3D-structured polymer network (Fig. 3). The elemental composition of the polymer was evaluated *via* EDS mapping analysis. It was found that the cryogel consisted of 54.77 wt.% carbon, 16.02 wt.% nitrogen, 24.95 wt/% oxygen, and 4.26 wt.% sodium. The detected sodium originated from the NaOH used in the synthesis of 4-VP-MAAc cryogel.

The swelling experiments showed that the 4-VP-MAAc cryogel was able to immediately adsorb water, with a swelling of 2100%. This fast swelling was due to the super-macroporous structure and the presence of hydrophilic functional groups.

Effect of pH

To evaluate the cryogel behavior at different pH environments, the zeta potential and MB removal were determined (Fig. 4). The cryogel was negatively charged in the whole range of pH values (Fig. 4(A)). This can be attributed to the protonation of carboxyl and sulphate groups from APS. At acidic pH, the zeta potential was around −12 mV due to the protonation of the pyridine groups of 4-VP.[33] The absolute zeta potential value increased to −33.4 mV at basic pH values possibly due to the start of protonation of carboxylate groups, while the presence of other acidic groups increased the negative charge of the polymer. Therefore, positively charged molecules could be adsorbed throughout the whole pH range, while increasing pH values further favored the adsorption capacity.

MB equilibrium adsorption results agreed with zeta potential observations; the adsorption of MB increased with increasing pH (Fig. 4(B)). At pH 1 and 2, 4-VP-MAAc removed ~57 mg/g, while with an increase in pH to 3, the maximum removal capacity drastically increased to 312.9 mg/g. With a further increase in pH, the q_{max} started to gradually increase and reached equilibrium at pH 7, with maximum removal capacity values ranging from 472.4–477.9 mg/g. At low pH, H^+ competes for the ion exchange sites of 4-VP-MAAc, preventing the absorption of MB. In addition, at higher pH values, an excess of hydroxyl ions can cause a strong electrostatic attraction of positively charged methylene blue molecules to negatively charged adsorption sites, and this causes a sudden increase in adsorption capacity.[34] Additionally, the concentrations of the released Na + from the cryogel to the solutions with different pH values, without adding MB, were analyzed. The results showed that concentrations of released sodium were in the range of 0.43–0.57 ppm, which are close to the values of pure DI water.

Table 2. Removal of MB by various materials

Type of adsorbent	Initial MB conc, mg/L	Initial pH	Removal mechanism	Maximum removal capacity, mg/g	Ref
P(NIPAAm/IA/Pumice)	150	7	Hydrogen bonding	8.9	45
Corn stalk/ montmorillonite cryogel	50	7	Chemisorption	49.0	39
Alginate/montmorillonite cryogel	1000	-	Ion-exchange	559.9	38
GO/alginate quasi-cryogel	1000	-	$\pi-\pi$ interaction	122.3	22
Vinyl hybrid silica hydrogel	350	7	Hydrogen bonding and complexation	1690	23
chitosan-g-poly(acrylic acid) /CNWs hydrogel	2000	6	Chemisorption	1968	46
p(NaVS-AMPS)/Fe_3O_4 cryogel	500	7	Ion exchange	780	36
p(AMPS-HEMA) cryogel	511	7.1	Chemisorption	1228	37
4VP-MAAc cryogel	50	6	Ion-exchange	703.6	This work

Table 3. Parameters of isotherm models for adsorption of MB by 4-VP-MAAc cryogel

Model name	Unit	Values
Experimental data	q_{max}^{exp} (mg/g)	703.6
Langmuir model	q_m (mg/g)	625.0
	K_L (L/mg)	0.0401
	R_L	0.9615
	R^2	0.9958
Freundlich model	1/n	0.6467
	K_F	29.5
	R^2	0.9786

Table 4. Parameters of breakthrough models for adsorption of MB by 4-VP-MAAc cryogel

Model name	Unit	Values
Experimental data	q_{exp} [mg/g]	388
Thomas model	k_{Th} [mL/mg min]	6.1×10^{-3}
	q_{Th} [mg/g]	342.7
	R^2	0.991
Adam-Bohart model	k_{AB} [mL/mg min]	6.1×10^{-1}
	N [mg/cm]	120.9
	R^2	0.937
Yoon-Nelson model	k_{YN} [mL/min]	2.6×10^{-1}
	τ [min]	29.7
	R^2	0.999

Adsorption kinetics

It is important to carry out both experimental adsorption kinetics and modelling of cryogels because these provide essential data on the dynamics of remediation, the efficiency of the cryogel, and the removal mechanism of removal. As shown in Fig. 5, the equilibrium removal of MB from water by the 4-VP-MAAc cryogel was achieved in 40 min. Specifically, a rapid increase of MB removal was observed in the first 10 min, while adsorption gradually progressed to 97 ± 2%.

To further evaluate the reaction kinetics, pseudo first/second order and second-order kinetics were applied, as shown in Table 1. Pseudo-second order kinetics better described and fit the adsorption performance of the cryogel. The model provided an adsorption capacity of 526.3 mg/g against the experimental one of 516.1 mg/g, with a correlation coefficient R^2 of 0.9998.

The pseudo-second order kinetics diffusion coefficient, k_2, corresponded to 1.0×10^{-3} g/mg min, which agrees with the experimental observations; it also demonstrated a relatively rapid removal during the first 20 min that smoothly decelerated towards the maximum removal capacity or saturation. Although the pseudo-first order kinetics modelling displayed close values in terms of diffusion coefficient (1.8×10^{-3} g/mg/min), it failed to fit the experimental adsorption capacity index since the discrepancy factor d_f ($q_{eq}^{cal}/q_{eq}^{exp}$) between these two was approximately 0.49. The results obtained were like those previously reported on different types of cryogels used for MB removal from water.[35-37] Hence, it is assumed that the pseudo-second order model better describes and fits the experimental results; it might also be applicable for macroporous materials with a high diffusion profile, such as cryogels. The proposed adsorption mechanisms linked with the adsorption equilibrium performance are discussed in section 3.6.

Adsorption equilibrium

To elaborate on the adsorption performance of the cryogel, the batch adsorption isotherm was studied (Fig. 6). The 4-VP-MAAc cryogel had an equilibrium adsorption capacity of 703.6 mg/g, which is comparable with similar polymer-based hydrogels and cryogels studied for MB removal from water, as shown in Table 2.

For example, Sezen *et al.*[38] recently prepared a composite of alginate and montmorillonite based cryogels by a one-step cryogelation technique that demonstrated an adsorption capacity of 559.94 mg/g. Similarly, Balkiz *et al.*[22] synthesized graphene oxide-alginate based quasi-cryogels that were produced *via* an effective quasi-cryogelation method, wherein the observed maximum adsorption capacity was 122.26 mg/g. On the other hand, Ma *et al.*[39] produced hydrogels *via* an aqueous solution polymerization approach under ultrasonic treatment with functional monomers and organic montmorillonite, but the adsorption capacity was considerably lower at 49.01 mg/g.

Both Langmuir and Freundlich models demonstrated acceptable correlation coefficients: 0.9958 and 0.9786, respectively (Table 3). However, the Langmuir isotherm model provided an adsorption capacity equal to 625 mg/g, which is close to the experimental value of 703.6 mg/g. Therefore, it could be suggested that the adsorption of MB onto cryogel followed the Langmuir model, thus indicating monolayer adsorption. The high value of K_L (0.0401) indicated a high rate of adsorption of dye on the cryogel, while the separation factor (R_L) value of 0.9615 denoted a favorable adsorption. These results agreed with the adsorption kinetics, where rapid adsorption was observed at the beginning with a gradual decline over time that could be possibly

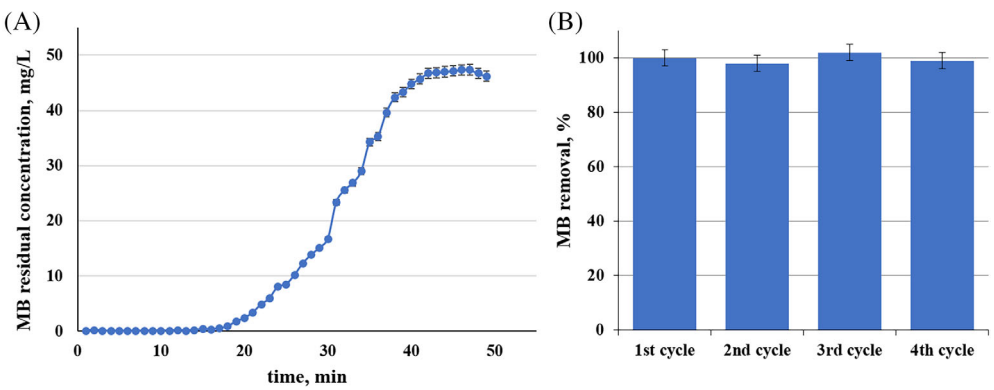

Figure 7. Breakthrough curve for 4VP-MAAc cryogel (A) and MB removal during four adsorption/desorption cycles (B).

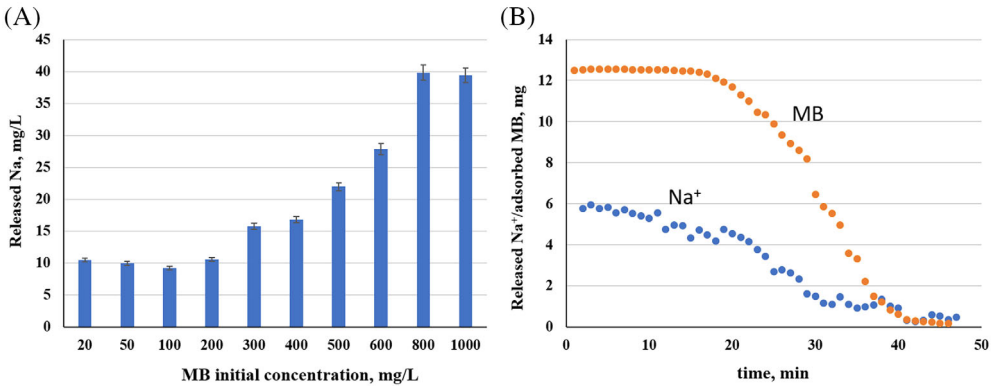

Figure 8. Concentration of released Na^+ ions at various concentrations of MB (A) and mass of released Na^+ *vs* adsorbed MB *vs*. time (B).

related to the saturation of the monolayer. Even though the Freundlich model did not fit the experimental data as efficiently as the Langmuir model, it led to the same qualitative conclusions; the value 0.6467 of 1/n lying between 0.1 and 1 also indicated a favorable adsorption, while the high K_F value of the model suggested an easy adsorption of MB from water.[40]

Similar studies on cryogels modified with magnetite nanoparticles[36] and cryogelic composites based on alginate/montmorillonite[38] have also indicated that the Langmuir model better described the adsorption of MB in the macroporous structure. These modified cryogel and cryogelic composites displayed a high degree of fitting in the Langmuir model. Dragan and Loghin[41] synthesized cryogels *via* radical polymerization in the presence of anionic polyelectrolytes derived from potato starch. According to their findings, the Langmuir model showed a good agreement with the experimental values, revealing a maximum adsorption capacity of 639 mg/g and a correlation coefficient of 0.979. Zhou *et al.*[42] produced a nanocomposite of polyacrylamide/cellulose nanocrystals impregnated into a hydrogel matrix *via* a partial hydrolysis reaction. The produced nanocomposite also showed a high degree of fitting with the Langmuir isotherm model (correlation coefficient of 0.997), with the experimental and calculated adsorption capacities being 326.08 and 358.42 mg/g, respectively. These results were supported by the regeneration experiments of MB-loaded cryogels, which are presented in the next paragraph (Table 3).

Fixed-bed column and regeneration/reusability study

A fixed bed column was used for studying the dynamic sorption of cryogel and the results are shown in Fig. 7(A), as the dependence of the residual dye concentration at the outlet of the column *versus* the process time. The data show that during the first

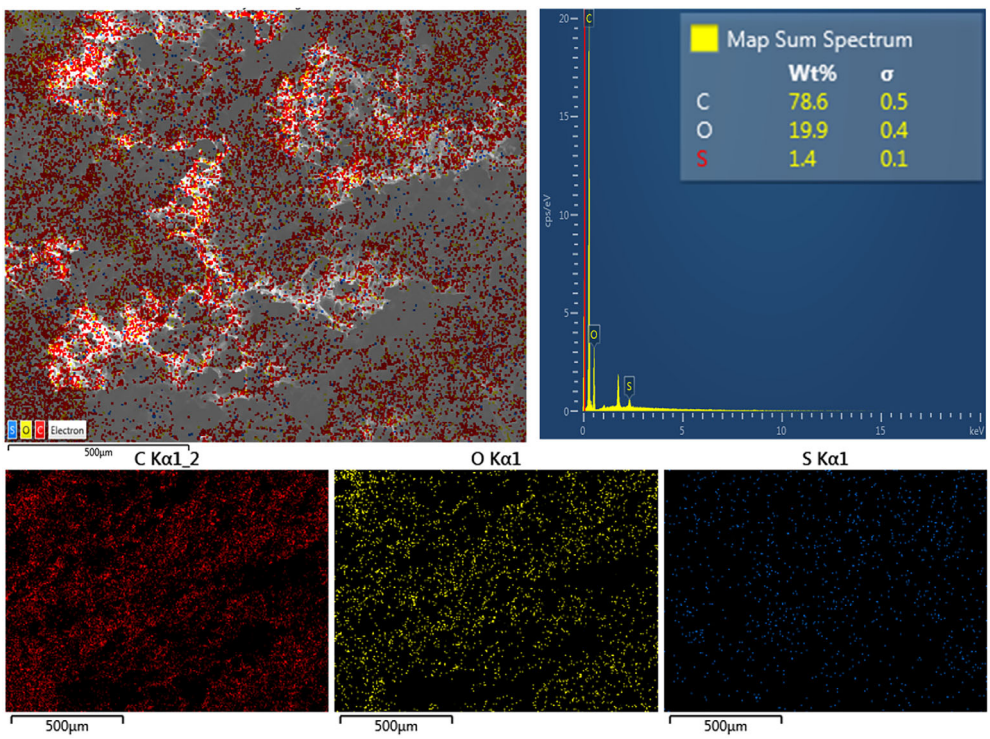

Figure 9. EDS mapping images of elemental composition (Carbon: red dots, Oxygen: yellow dots, Sulfur: blue dots) of MB-adsorbed 4VP-MAAc cryogel.

18 min of the 50 ppm methylene blue solution flow through the cryogel (at a rate of 8 mL per minute), the cryogel adsorbed all of the passing dye. As the polymer was saturated with the dye, the concentration of the non-adsorbed MB gradually increased, with complete saturation of the sample being observed after approximately 45 min.

The proper configuration and operation of a fixed-bed column system requires the prediction of the breakthrough curve for the adsorbate. Therefore, the breakthrough curve for the removal capacity of the cryogel was studied using the Thomas, Adams–Bohart, and Yoon–Nelson models by applying linear regression analysis. The comparison between the obtained model parameters and the experimental values of adsorption capacity are presented in Table 4.

The correlation coefficient for the Thomas and Yoon–Nelson models were nearly comparable (0.991 and 0.999, respectively), and higher than the values obtained for the Adams–Bohart model ($R^2 = 0.937$). The adsorption capacity calculated by means of the Thomas model was close to the experimental value. According to the Yoon-Nelson model, the half time of the breakthrough is 29.7 min.

Regeneration and reuse of the adsorbent for several cycles is one of the most important aspects from an economic point of view when using adsorbents on an industrial scale. The MB removal efficiency of the cryogel after each of the four successive cycles is shown in Fig. 7(B). It is clear that the desorption/adsorption process was effective in all four cycles, with the adsorption capacity remaining at almost 100% in all cases.

Mechanisms of removal

One of the proposed removal mechanisms involves the ion exchange process between H^+ and/or Na^+ in the cryogel phase with MB^+ from the solution phase, along with van der Waals force and hydrogen bonding interactions with the functional groups. The trends of the release of Na^+ ions and adsorption of MB at different initial dye concentrations are presented in Fig. 8(A). At low dye concentrations, a small release of sodium ions was observed, while at full saturation, the concentration of the released sodium ions also increased. These findings were also proven in fixed-bed column experiments (Fig. 7(A)), where the curve of the released Na^+ ions had a similar shape as that of the adsorbed MB (Fig. 8 (B)), showing that ion-exchange of sodium with MB was the main removal mechanism.

The EDS mapping (Fig. 9) of cryogel after the MB removal also confirmed the disappearance of sodium ions from the surface of the cryogel with the simultaneous appearance of sulfur and increased content of carbon coming from the MB structure.

Despite the ion-exchange mechanism of Na^+/MB^+ interaction, the molar ratio of the released sodium and dye was not equal. The other possible mechanism of adsorption is the complexation of positively charged MB with the functional groups of the polymer.

The FT-IR spectrum of MB-loaded cryogel in comparison with that of the pure polymer was provided in Fig. 2. It can be clearly observed that –OH stretching frequency at ~3300 cm^{-1} at the parent cryogel shifted to lower frequencies (~3240 cm^{-1}), indicating the interaction of MB with the surface of the cryogel. The peak of amide(I) group at 1600 cm^{-1} in 4-VP-MAAc was shifted to lower frequencies by 18 cm^{-1} with an increase in the intensity of MB-adsorbed cryogel. Additionally, the peak of –OH bending coming from carboxylic acid group was shifted from 1398 to 1386 cm^{-1} due to the interaction of the positively charged dye with the negatively charged functional groups.[43,44]

CONCLUSIONS

A novel macroporous 4-vinylpyridine-co-methacrylic acid-based cryogel was synthesized, characterized, and studied in the removal of methylene blue dye from water. The results of batch adsorption kinetics showed a rapid removal of dye of around 90% within the first 20 min that reached almost 100% in the next 10 min, corresponding to an equilibrium capacity of 516.1 mg/g. The experimental results were well described by a pseudo-second order kinetics model.

Fixed-bed column experiment results revealed that the obtained cryogel could be used in four successive adsorption/desorption cycles without any loss of adsorption capacity. The MB removal was found to take place through an ion exchange and complexation reaction with functional groups of polymer mechanism.

ACKNOWLEDGEMENTS

This research was funded by the Science Committee of the Ministry of Education and Science of the Republic of Kazakhstan (Grant No. AP09259907).It was also supported by the EU-funded project *'Nanoporous and Nanostructured Materials for Medical Applications (NanoMed)'*, H2020-MSCA-RISE-2016, 734641. Dr. S. G. Poulopoulos acknowledges the financial support from the Nazarbayev University project 'Cost-Effective Photocatalysts for the Treatment of Wastewaters containing Emerging Pollutants', Faculty Development Competitive Research Grants Program for 2020–2022, Grant Number 240919FD3932.

REFERENCES

1 *Textiles and Clothing*, 1st edn. Scrivener Publishing LLC, Beverly, Massachusetts, USA. (2019) https://onlinelibrary.wiley.com/doi/10.1002/9781119526599#page=24.
2 Starovoytova D. Assessment of toxicity of textile dyes and chemicals via Materials Safety Data Sheets 2014. https://www.researchgate.net/profile/Diana-Starovoytova/publication/309155638_Assessment_of_Toxicity_of_Textile_Dyes_and_Chemicals_via_Materials_Safety_Data_Sheets/links/5801550008ae1c5148c9fded/Assessment-of-Toxicity-of-Textile-Dyes-and-Chemicals-via-Mat.
3 Osman M, Waste water treatment in chemical industries: the concept and current technologies. *Hydrol Curr Res* **05**:164 (2014). https://doi.org/10.4172/2157-7587.1000164.
4 Rastogi K, Sahu JN, Meikap BC and Biswas MN, Removal of methylene blue from wastewater using fly ash as an adsorbent by hydrocyclone. *J Hazard Mater* **158**:531–540 (2008).
5 Singh P, Sharma K, Hasija V, Sharma V, Sharma S, Raizada P *et al*., Systematic review on applicability of magnetic iron oxides–integrated photocatalysts for degradation of organic pollutants in water. *Mater Today Chem* **14**:100186 (2019).
6 Ahmad R and Kumar R, Adsorption studies of hazardous malachite green onto treated ginger waste. *J Environ Manage* **91**:1032–1038 (2010).
7 Wang L, Zhang J and Wang A, Removal of methylene blue from aqueous solution using chitosan-g-poly(acrylic acid)/montmorillonite superadsorbent nanocomposite. *Colloids Surf A: Physicochem Eng Asp* **322**:47–53 (2008).
8 Kasperchik VP, Yaskevich AL and Bil'dyukevich AV, Wastewater treatment for removal of dyes by coagulation and membrane processes. *Pet Chem* **52**:545–556 (2012).
9 Chiu Y-H, Chang T-FM, Chen C-Y, Sone M and Hsu Y-J, Mechanistic insights into photodegradation of organic dyes using heterostructure photocatalysts. *Catalysts* **9**:430 (2019).
10 Liang C-Z, Sun S-P, Li F-Y, Ong Y-K and Chung T-S, Treatment of highly concentrated wastewater containing multiple synthetic dyes by a

combined process of coagulation/flocculation and nanofiltration. *J Membr Sci* **469**:306–315 (2014).
11 Senthil Kumar P, Joshiba GJ, Femina CC, Varshini P, Priyadharshini S, Arun Karthick MS *et al*., A critical review on recent developments in the low-cost adsorption of dyes from wastewater. *Desalin Water Treat* **172**:395–416 (2019).
12 Joseph J, Radhakrishnan RC, Johnson JK, Joy SP and Thomas J, Ion-exchange mediated removal of cationic dye-stuffs from water using ammonium phosphomolybdate. *Mater Chem Phys* **242**:122488 (2020).
13 Collivignarelli MC, Abbà A, Carnevale Miino M and Damiani S, Treatments for color removal from wastewater: state of the art. *J Environ Manage* **236**:727–745 (2019).
14 Wu Z, Zhong H, Yuan X, Wang H, Wang L, Chen X *et al*., Adsorptive removal of methylene blue by rhamnolipid-functionalized graphene oxide from wastewater. *Water Res* **67**:330–344 (2014).
15 Ishak SA, Murshed MF, Md Akil H, Ismail N, Md Rasib SZ and Al-Gheethi AAS, The application of modified natural polymers in toxicant dye compounds wastewater: A review. *Water* **12**:2032 (2020).
16 Wong S, Ngadi N, Inuwa IM and Hassan O, Recent advances in applications of activated carbon from biowaste for wastewater treatment: A short review. *J Clean Prod* **175**:361–375 (2018).
17 Roshanfekr Rad L and Anbia M, Zeolite-based composites for the adsorption of toxic matters from water: A review. *J Environ Chem Eng* **9**:106088 (2021).
18 Kausar A, Iqbal M, Javed A, Aftab K, Nazli Z-H, Bhatti HN *et al*., Dyes adsorption using clay and modified clay: A review. *J Mol Liq* **256**: 395–407 (2018).
19 Ates B, Koytepe S, Ulu A, Gurses C and Thakur VK, Chemistry, structures, and advanced applications of nanocomposites from biorenewable resources. *Chem Rev* **120**:9304–9362 (2020).
20 Baimenov A, Berillo DA, Poulopoulos SG and Inglezakis VJ, A review of cryogels synthesis, characterization and applications on the removal of heavy metals from aqueous solutions. *Adv Colloid Interface Sci* **276**:102088 (2020). https://doi.org/10.1016/j.cis.2019.102088.
21 Wan W, Bannerman AD, Yang L and Mak H, Poly(vinyl alcohol) Cryogels for biomedical applications, in *Polymeric Cryogels: Macroporous Gels with Remarkable Properties*, ed. by Okay O. Springer International Publishing, Cham, pp. 283–321 (2014).
22 Balkız G, Pingo E, Kahya N, Kaygusuz H and Bedia EF, Graphene oxide/alginate quasi-Cryogels for removal of methylene blue. *Water Air Soil Pollut* **229**:131 (2018).
23 Chen M, Shen Y, Xu L, Xiang G and Ni Z, Highly efficient and rapid adsorption of methylene blue dye onto vinyl hybrid silica nano-cross-linked nanocomposite hydrogel. *Colloids Surf A: Physicochem Eng Asp* **613**:126050 (2021).
24 Wang W, Zhao Y, Bai H, Zhang T, Ibarra-Galvan V and Song S, Methylene blue removal from water using the hydrogel beads of poly(vinyl alcohol)-sodium alginate-chitosan-montmorillonite. *Carbohydr Polym* **198**:518–528 (2018).
25 Baimenov A, Berillo D, Azat S, Nurgozhin T and Inglezakis V, Removal of cd^{2+} from water by use of super-macroporous cryogels and comparison to commercial adsorbents. *Polymers* **12**:1–19 (2020). https://doi.org/10.3390/polym12102405.
26 Taşdelen B, Çifçi Dİ and Meriç S, Preparation and characterization of chitosan/AMPS/kaolinite composite hydrogels for adsorption of methylene blue. *Polym Bull* (2021). https://doi.org/10.1007/s00289-021-03970-w.
27 Ho YS and McKay G, Pseudo-second order model for sorption processes. *Process Biochem* **34**:451–465 (1999).
28 Ge H and Hua T, Synthesis and characterization of poly(maleic acid)-grafted crosslinked chitosan nanomaterial with high uptake and selectivity for hg(II) sorption. *Carbohydr Polym* **153**:246–252 (2016).
29 Langmuir I, The constitution and fundamental properties of solids and liquids. Part I. solids. *J Am Chem Soc* **38**:2221–2295 (1916).
30 Hayati B, Maleki A, Najafi F, Gharibi F, McKay G, Gupta VK *et al*., Heavy metal adsorption using PAMAM/CNT nanocomposite from aqueous solution in batch and continuous fixed bed systems. *Chem Eng J* **346**:258–270 (2018).
31 Wang X, Deng W, Xie Y and Wang C, Selective removal of mercury ions using a chitosan–poly(vinyl alcohol) hydrogel adsorbent with three-dimensional network structure. *Chem Eng J* **228**:232–242 (2013).
32 Sumesh E, Bootharaju MS and Anshup PT, A practical silver nanoparticle-based adsorbent for the removal of Hg2+ from water. *J Hazard Mater* **189**:450–457 (2011).
33 Ito M, Takano K, Hanochi H, Asaumi Y, Yusa S-I, Nakamura Y *et al*., pH-responsive aqueous bubbles stabilized with polymer particles carrying poly(4-vinylpyridine) colloidal stabilizer. *Front Chem* **6**:269 (2018).
34 Mouni L, Belkhiri L, Bollinger J-C, Bouzaza A, Assadi A, Tirri A *et al*., Removal of methylene blue from aqueous solutions by adsorption on kaolin: kinetic and equilibrium studies. *Appl Clay Sci* **153**:38–45 (2018).
35 Atta AM, Al-Lohedan HA, Tawfeek AM and Ahmed MA, In situ preparation of magnetic Fe3O4.Cu2O.Fe3O4/cryogel nanocomposite powder via a reduction–coprecipitation method as adsorbent for methylene blue water pollutant. *Polym Int* **67**:925–935 (2018).
36 Al-Hussain SA, Atta AM, Al-Lohedan HA, Ezzat AO and Tawfeek AM, Application of new sodium vinyl sulfonate–co-2-Acrylamido-2-me [thylpropane] sulfonic acid sodium salt-magnetite cryogel nanocomposites for fast methylene blue removal from industrial waste water. *Nanomaterials* **8**:878 (2018).
37 Atta AM, Ezzat AO, Al-Hussain SA, Al-Lohedan HA, Tawfeek AM and Hashem AI, New crosslinked poly (ionic liquid) cryogels for fast removal of methylene blue from waste water. *React Funct Polym* **131**:420–429 (2018).
38 Sezen S, Thakur VK and Ozmen MM, Highly effective covalently cross-linked composite alginate Cryogels for cationic dye removal. *Gels* **7**: 178 (2021).
39 Ma D, Zhu B, Cao B, Wang J and Zhang J, Fabrication of the novel hydrogel based on waste corn stalk for removal of methylene blue dye from aqueous solution. *Appl Surf Sci* **422**:944–952 (2017).
40 Tseng R-L and Wu F-C, Inferring the favorable adsorption level and the concurrent multi-stage process with the Freundlich constant. *J Hazard Mater* **155**:277–287 (2008).
41 Dragan ES and Apopei Loghin DF, Enhanced sorption of methylene blue from aqueous solutions by semi-IPN composite cryogels with anionically modified potato starch entrapped in PAAm matrix. *Chem Eng J* **234**:211–222 (2013).
42 Zhou C, Wu Q, Lei T and Negulescu II, Adsorption kinetic and equilibrium studies for methylene blue dye by partially hydrolyzed polyacrylamide/cellulose nanocrystal nanocomposite hydrogels. *Chem Eng J* **251**:17–24 (2014).
43 Uppal R, Incarvito CD, Lakshmi KV and Valentine AM, Aqueous spectroscopy and redox properties of carboxylate-bound titanium. *Inorg Chem* **45**:1795–1804 (2006).
44 Wu N, Fu L, Su M, Aslam M, Wong KC and Dravid VP, Interaction of fatty acid monolayers with cobalt nanoparticles. *Nano Lett* **4**:383–386 (2004).
45 Taşdelen B, Çifçi Dİ and Meriç S, Preparation of N-isopropylacrylamide/itaconic acid/pumice highly swollen composite hydrogels to explore their removal capacity of methylene blue. *Colloids Surf A: Physicochem Eng Asp* **519**:245–253 (2017).
46 Melo BC, Paulino FAA, Cardoso VA, Pereira AGB, Fajardo AR and Rodrigues FHA, Cellulose nanowhiskers improve the methylene blue adsorption capacity of chitosan-g-poly(acrylic acid) hydrogel. *Carbohydr Polym* **181**:358–367 (2018).